TISSUE ENGINEERING: Part A
Volume 18, Numbers 19 and 20, 2012

DOI: 10.1089/ten.tea.2011.0606

Anisotropic Fibrous Scaffolds for Articular Cartilage Regeneration

Seth D. McCullen, Ph.D., Hélène Autefage, Ph.D., Anthony Callanan, Ph.D., Eileen Gentleman, Ph.D., and Molly M. Stevens, Ph.D.

Articular cartilage lesions, which can progress to osteoarthritis, are a particular challenge for regenerative medicine strategies, as cartilage function stems from its complex depth-dependent microstructural organization, mechanical properties, and biochemical composition. Fibrous scaffolds offer a template for cartilage extracellular matrix production; however, the success of homogeneous scaffolds is limited by their inability to mimic the cartilage's zone-specific organization and properties. We fabricated trilaminar scaffolds by sequential electrospinning and varying fiber size and orientation in a continuous construct, to create scaffolds that mimicked the structural organization and mechanical properties of cartilage's collagen fibrillar network. Trilaminar composite scaffolds were then compared to homogeneous aligned or randomly oriented fiber scaffolds to assess *in vitro* cartilage formation. Bovine chondrocytes proliferated and produced a type II collagen and a sulfated glycosaminoglycan-rich extracellular matrix on all scaffolds. Furthermore, all scaffolds promoted significant upregulation of aggrecan and type II collagen gene expression while downregulating that of type I collagen. Compressive testing at physiological strain levels further demonstrated that the mechanical properties of trilaminar composite scaffolds approached those of native cartilage. Our results demonstrate that trilaminar composite scaffolds mimic key organizational characteristics of native cartilage, support *in vitro* cartilage formation, and have superior mechanical properties to homogenous scaffolds. We propose that these scaffolds offer promise in regenerative medicine strategies to repair articular cartilage lesions.

Introduction

Articular cartilage lesions, which can progress to osteoarthritis, are a particular challenge for regenerative medicine strategies, as cartilage function stems from its complex depth-dependent microstructural organization, mechanical properties, and biochemical composition.[1,2] Repairing such lesions with engineered scaffolds containing live cells before they progress to osteoarthritis therefore remains an important aim in the field of regenerative medicine. Articular cartilage is a highly organized, fiber-reinforced tissue that provides a low-friction and wear-resistant-bearing surface in diarthrodial joints.[2,3] Articular cartilage exhibits anisotropic mechanical properties as a result of depth-dependent differences in the density and structural arrangement of its extracellular matrix, which consists predominantly of proteoglycan molecules retained within a fibrillar type II collagen meshwork.[3] The fibrillar collagen meshwork provides mechanical reinforcement and is comprised of three zones, namely the superficial, middle, and deep zones.[2] As a function of these zones, collagen fibers vary in their alignment, progressing from parallel in the superficial region, to random in the middle zone, and finally orientating perpendicular to the subchondral bone surface in the deep zone.[3] This anisotropic fiber orientation contributes to depth-dependent or zonal mechanical properties in terms of ultimate tensile strength and tensile modulus.[2,3]

A number of strategies have been explored for articular cartilage repair, including the use of synthetic polymer fleeces, sponges, and fibrous materials that can be seeded with a patient's own chondrocytes or stem cells and either sutured or packed into defect sites.[4,5] Although such therapies can promote the formation of neocartilagenous tissue *in vivo*, their homogenous design likely limits successful outcomes. Regenerated tissue tends to suffer from marginal integration with the surrounding cartilage and poor mechanical properties arising from the production of fibrocartilage, both of which may be attributable to the lack of native tissue-like structure and organization within such scaffolds.[4] Therefore, in an effort to mimic the fibrillar network of articular cartilage, electrospun scaffolds comprised of fibers with diameters on the micron-to-submicron size scale have also been explored, as these materials are able to mimic natural cell–extracellular matrix interactions, promote production of cartilage-like tissue, and provide a template to organize the newly deposited matrix.[6–8]

Departments of Materials and Bioengineering, Institute of Biomedical Engineering, Imperial College London, London, United Kingdom.

Electrospinning is a facile technique capable of generating dense, compliant, biocompatible fiber networks with tunable physical properties such as fiber size, spacing, orientation, and tensile properties.[9,10] Fiber size, in particular, plays a crucial role in determining the mechanical properties of the bulk scaffold. By varying the fiber size, the resultant pore size and mechanical strength can be varied over a wide range.[10,11] In addition, fiber orientation can be varied by modifying collector geometry or rotating collector speed, yielding fibrous scaffolds that vary from randomly oriented scaffolds to highly aligned networks with concomitant variations in tensile strength.[9,12,13] Nevertheless, such homogenous, electrospun scaffolds still lack cartilage's zonal organization, and are therefore unable to regenerate this native tissue's anisotropic mechanical properties, collagen fiber orientation, biochemical gradients, and cellular distribution.[14,15]

Biodegradable scaffolds that are functionally graded in terms of organization, porosity, pore size, and mechanical properties may provide distinct advantages over scaffolds that feature uniform properties and homogeneous compositions.[2,16] Specifically, scaffolds with depth-dependent variations in the fibrillar size and orientation that mimic the composition and structure of the native tissue may offer a superior template for cellular organization and extracellular matrix production. A technique to incorporate multiple electrospun layers with distinct fiber sizes and orientations is that of sequential electrospinning onto the same collector under varying operating conditions.[17] This method has been employed to create bilaminar, trilaminar, and multilayer scaffolds to repair blood vessels,[17–19] but to our knowledge, has not been investigated in recreating the zonal organization of structurally supportive tissues such as articular cartilage.

Herein, we generate trilaminar electrospun scaffolds by varying both the fiber size and orientation to create scaffolds that mimic both the fiber orientation and the zonal tensile properties of articular cartilage. Trilaminar composite electrospun scaffolds were directly compared with homogenous scaffolds formed from either randomly oriented or aligned fibers in terms of their compressive mechanical properties and the ability to support *in vitro* cartilage formation. Our results demonstrate that trilaminar composite scaffolds mimic a number of key organizational characteristics of native cartilage, support *in vitro* cartilage formation, and have superior mechanical properties to homogenous scaffolds, demonstrating their promise in regenerative medicine strategies to repair articular cartilage lesions.

Materials and Methods

Scaffold fabrication

Poly(ε-caprolactone) (PCL) with a number average M_n, molecular weight of 80,000 Da, and the solvent 1,1,1,3,3,3-hexafluoroisopropanol (HFIP) were procured from Sigma-Aldrich. Fibrous scaffolds were fabricated on a custom-made electrospinning setup that included a programmable syringe pump (Kd Scientific Model KDS 100 CE; Sandbach), a Glassman high voltage power supply series WR (Glassman; Bramley), and a voltage-driven rotating mandrel. Scaffolds of varying fiber size were fabricated by dissolving PCL in HFIP at either 15 or 25 wt% overnight and then electrospinning the solution through a 16-gauge blunt-tip needle collected onto a rotating mandrel (width = 6 cm; diameter = 20 cm) at a linear velocity of either 0–1 or 20 m/s. To fabricate trilaminar scaffolds, 10 mL of a 15 wt% PCL solution was electrospun and collected at a linear velocity of 20 m/s, followed by a second 10-mL volume of 15 wt% PCL collected at 0–1 m/s, and a final 10-mL volume of 25 wt% PCL collected at 0–1 m/s.

Scaffold characterization using electron microscopy

Scaffolds were imaged using a JEOL 5610 (Herts) environmental scanning electron microscope (SEM). Specimens were coated with 100Å Au using an Emitech K550 sputter coater and observed at an accelerating voltage of 20 kV and a working distance of 10 cm. The fiber size and pore size were determined from 10 representative images using NIH ImageJ Software (NIH). The pore size was estimated by measuring the void space between fiber interstices. The scaffolds were cross-sectionally examined by SEM after freeze-fracturing the scaffolds immersed in liquid nitrogen.

Mechanical testing of scaffolds

Homogenous (randomly oriented and aligned) and trilaminar composite scaffolds were mechanically tested in tension to failure using an Instron Model 5540 testing machine (Norwood), equipped with a 50-N load cell operated at a crosshead speed of 10 mm/min. Specimens had a gauge length of 30 mm and width of 10 mm; the thickness was measured by digital calipers and confirmed by SEM. Ultimate tensile strength and Young's modulus were determined from stress–strain curves, where the ultimate tensile strength was taken as the maximum stress, and the Young's modulus was calculated from the linear region of the stress–strain curve.

Compressional mechanics of scaffolds was measured in unconfined uniaxial compression testing using an Instron Model 5540 testing machine equipped with a 10-N load cell. Three-mm-diameter samples were cored from 10-mm-diameter samples, preloaded to 0.07 N, allowed to equilibrate for 5 min, and then compressed to 10% strain at a crosshead speed of 0.5% strain/min as previously reported.[20] Tangent modulus and peak stress were calculated from the linear portion of the stress–strain curve, and the maximum stress level was achieved (minus the preload), respectively.

Bovine chondrocyte isolation

Bovine cartilage was harvested from the lower leg joint of young calves. Briefly, the ankle joint was cut open along the joint line, and cartilage tissue was cut with a scalpel into thin sections parallel to the subchondral bone. Chondrocytes were isolated by digesting in the Dulbecco's modified Eagle's medium (DMEM) + glutamax (4.5 g/L glucose) with 0.2% w/v pronase, 10 mM HEPES, 50 μg/mL gentamicin (all reagents from Invitrogen) for 1 h at 37°C with agitation. This digest was removed and replaced with DMEM + glutamax (4.5g/L glucose) supplemented with 10 mM HEPES, 50 μg/mL gentamicin, 5% v/v fetal bovine serum (FBS) (Invitrogen) and 0.04% w/v collagenase type I (Sigma) overnight at 37°C with agitation. After digestion, isolated chondrocytes were filtered through a 70-μm pore size filter, centrifuged at

250 g for 3 min, and plated in the DMEM (4.5g/L glucose) with 10% v/v FBS, 50 μg/mL ascorbic acid (Sigma), and 50 μg/mL gentamicin (expansion medium).

Assessment of in vitro *chondrogenesis*

Trilaminar composite scaffolds were compared directly to scaffolds comprised of fully randomly oriented or aligned fibers with fiber diameters of 1 μm (30-mL total solution volume) collected at 1 or 20 m/s, respectively. All scaffolds were ~1 mm in thickness. Before chondrocyte seeding, 10-mm-diameter scaffolds were punched from electrospun sheets. Scaffolds were sterilized in 70% ethanol for 30 min followed by three washes with sterile phosphate-buffered saline (PBS) and then soaked in 0.01% v/v bovine serum albumin (Sigma) in PBS overnight to assist with chondrocyte adhesion. Twenty microliters of expansion medium containing 0.25 M bovine chondrocytes (passage 1) was placed on one side of each scaffold, and cells were allowed to adhere for 2 h before seeding the other side with an additional 0.25 M chondrocytes. After chondrocyte adhesion, fibrous scaffolds were transferred to nonadherent 24-well plates and cultured in 1 mL of chondrogenic differentiation medium consisting of the DMEM (4.5 g/L l-glucose), supplemented with 50 μg/mL L-proline (Sigma), 50 μg/mL ascorbic acid (Sigma), 0.1 mM sodium pyruvate (Sigma), 10 ng/mL TGF-β3 (Lonza), and 1% v/v ITS Premix (BD Biosciences) at 37°C and 5% CO_2. The medium was changed twice weekly.

Chondrocyte viability, morphology, and biochemical assessment

Chondrocyte viability on electrospun scaffolds was assessed using the LIVE/DEAD® Cell Viability assay (Invitrogen) after 0, 1, 3, and 5 weeks in culture. Fibrous scaffolds were rinsed twice with PBS and incubated with 4 μM Calcein AM and 4 μM ethidium homodimer-1 in PBS, which stain live and dead cells green and red, respectively. Chondrocytes were imaged using an Olympus IX51 epifluorescence microscope equipped with an Olympus DP70 camera.

Chondrocyte morphology on electrospun scaffolds was assessed by examining the cytoskeletal organization by immunostaining. Scaffolds were fixed in 4% w/v paraformaldehyde for 15 min, washed twice with PBS, and permeabilized with 0.25% v/v Triton X-100 in PBS for 15 min. Actin cytoskeleton was stained with Alexa Fluor® 568 phalloidin (Invitrogen; 1:160) for 20 min, and nuclei were stained with DAPI (Sigma; 1:1000) for 2 min. Type I collagen and type II collagen were detected using collagen I antibody (rabbit polyclonal, Ab34710) and collagen II antibody (dilution ratio 1:100, rabbit polyclonal, Ab34712; Abcam). Both antibodies were detected using goat polyclonal secondary antibody to rabbit IgG with an FITC conjugation (Ab97050) (dilution ratio 1:1000) and counterstained with DAPI (Sigma; 1:1000) for 2 min. Sections were stained separately for collagens. Chondrocytes were imaged on an Olympus IX51 epifluorescence microscope equipped with an Olympus DP70 camera.

After 0, 1, 3, and 5 weeks of culture, chondrocyte-seeded scaffolds were digested in a papain digest (2.5 units papain/mL, 5 mM cysteine HCl, and 5 mM EDTA, in PBS [all reagents from Sigma]) at 60°C overnight. Digested samples were assayed for total DNA content using the Quant-iT™ PicoGreen® kit (Invitrogen), according to the manufacturer's instructions. Sulfated glycosaminoglycan (GAG) contents were determined using the Blyscan Kit (Biocolor), as per the manufacturer's instructions.

Histological examination of chondrocyte-seeded scaffolds

After 5 weeks in culture, fibrous scaffolds were embedded in the Tissue-Tek® OCT (Fischer Scientific) freezing medium and flash frozen in isopentane. Scaffolds were sectioned at 10 μm and stained for deposited sulfated proteoglycans (GAGs) using 0.1 wt% Alcian Blue (pH 1) or for collagen with Picrosirius Red (both from Sigma).

Gene expression analysis

After weeks 0, 1, 3 and 5, total RNA was isolated from the scaffolds using an RNeasy kit, and cDNA was obtained from reverse transcription using the QuantiTect Reverse Transcription kit (all from Qiagen). Real-time quantitative polymerase chain reaction (qPCR) was carried out on a Rotorgene Corbett PCR, using previously published primer sequences. qPCRs were performed on Glyceraldehyde-3-phosphate dehydrogenase (*GAPDH*) (*U85042*, forward: ACCCTCAA GATTGTCAGCAA, reverse: ACGA TGCCAAAGTGGTCA), Aggrecan (*ACAN, AGC1*) (U76615, forward: GCTACCCT-GACCCTTCATC, reverse: AAGCTTTCTGGGA TGTCCAC), *COL1A1* (NM-174520, forward: CATTAGGGGTCACAATG GTC, reverse: TGGAGTTCCA TTTTCACCAG), and *COL2A1* (X02420, forward: CATCCCACCCTCTCACAGTT, reverse: GTCTCTGCCTTGACCCAAAG) by using the QuantiTect SYBR Green PCR kit in accordance with the manufacturer's recommendations (Qiagen). Primers were validated, and the efficiencies of the primers have been found between 0.90 and 1.07. The gene expression levels were normalized to the expression of the housekeeping gene *GAPDH* and were expressed as fold changes relative to week-0 control samples. The relative mRNA levels of *ACAN*, *COL2A1*, and *COL1A1* were calculated using the ΔΔCt method, and the *COL2A1*/*COL1A1* ratio corresponds to the $2^{-\Delta Ct}$ of each gene.

Mechanical testing of chondrocyte-seeded scaffolds

After 5 weeks in culture, chondrocyte-seeded scaffolds were assessed for tensile and compressional properties, as previously described (Mechanical testing of scaffolds section). Additionally, separate fibrous scaffolds from matching samples were compressed to strains of up to 30% after a preload of 0.07N for 5 min. Segmental compressive moduli were calculated from stress–strain curves for 10% strain increments from 0%–10%, 10%–20%, and 20%–30%. Linearity for segmental compressive moduli possessed an $R^2 > 0.95$. Controls from bovine cartilage were cored and assessed in the same manner.

Statistical analysis

All experimental groups had a sample size of at least $n = 4$ for biochemical, qPCR, and histological analyses, and $n \geq 5$ for mechanical property analyses. Data are presented as average ± standard error mean. Statistical significance was

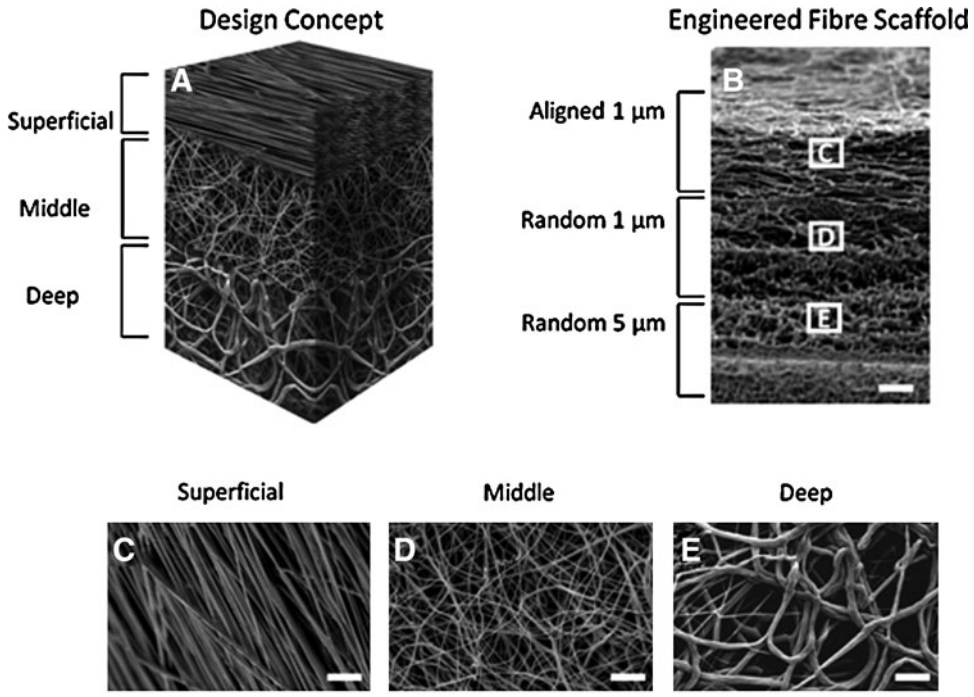

FIG. 1. Sequential electrospinning of poly(ε-caprolactone) at varying concentrations and collecting conditions was performed to generate dense fiber networks that preserve zonal fiber mechanical properties in a continuous scaffold. The diagram **(A)** illustrates the zonal placement of varying fiber zones and the resultant electron microscopy images of the bulk anisotropic scaffold **(B)** and the varying fibers of aligned 1-μm **(C)**, randomly oriented 1-μm **(D)**, or randomly oriented 5-μm fibers throughout the scaffold **(E)**. Scale bar = 100 μm in **(B)** and 10 μm in **(C–E)**.

determined by performing ANOVA and Turkey HSD tests with a significance accepted at a p-value < 0.05.

Results

Scaffold fabrication and characterization

To generate trilaminar composite scaffolds that featured a depth-dependent fiber organization and mechanical properties that mimicked those of native cartilage, we performed sequential electrospinning by varying both polymer concentration and collection conditions (Fig. 1). While varying the linear velocity of the collector from 20 to 1 m/s did not significantly alter fiber size (1.1 ± 0.3 vs. 0.9 ± 0.2 μm; Table 1), resulting fibers were either aligned or randomly oriented as determined by SEM (Fig. 1). Varying polymer concentration in solution from 15 to 25% w/v, however, significantly increased the fiber size from 0.9 ± 0.2 to 4.6 ± 1.2 μm and a resulting pore size from 12.9 ± 1.3 to 171 ± 102 μm^2 (Table 1). Tensile testing demonstrated that scaffolds produced with larger fiber diameters (5 μm) also displayed significantly lower ultimate tensile strengths and tensile moduli compared to scaffolds with smaller diameter fibers (1 μm) (Table 2). Conversely, scaffolds composed of aligned fibers had significantly higher tensile properties compared to either scaffolds composed of randomly oriented fibers of the same or larger diameters (Table 2). Trilaminar composite scaffolds displayed significantly higher ultimate tensile strengths than homogeneous randomly oriented fiber scaffolds of either 1 or 5 μm in diameter, yet their tensile moduli were not significantly different (Table 2).

Effect of scaffold design on the attachment, proliferation, and differentiation of bovine chondrocytes

We next evaluated the ability of bovine chondrocytes to adhere, proliferate, and differentiate on homogenous (aligned and randomly oriented with 1-μm fiber diameters; Fig. 2A and B, respectively) and trilaminar composite scaffolds (Fig. 2C, D). LIVE/DEAD Cell Viability assay demonstrated high cell viability throughout the 5 weeks for all scaffolds (Fig. 2E–H). Chondrocytes assumed an aligned morphology on aligned fibrous scaffolds and the aligned fiber side of trilaminar composite scaffolds (Fig. 2I, K).

Table 1. Electrospinning Parameters and Fiber Properties (Fiber Size and Resultant Pore Size) for Individual Electrospun Layers

Electrospun cartilage equivalent	*Polymer concentration (%w/v)*	*Working distance (cm)*	*Linear velocity (m/s)*	*Fiber orientation*	*Fiber size (μm)*	*Pore size (μm)*
Superficial	15	10	20	Aligned	1.1 ± 0.3	4.2 ± 1
Middle	15	10	0–1	Random	0.9 ± 0.2	12.9 ± 1.3
Deep	25	15	0–1	Random	4.6 ± 1.2	171 ± 102

All poly(ε-caprolactone) solutions were electrospun at an applied voltage of 15 kV and at a volumetric flow rate of 3 mL/h. Fiber size was preserved at varying linear velocities (20 vs. 1 m/s) at a constant polymer concentration (15% w/v), but significantly increased with the polymer concentration (15 vs. 25% w/v).

Table 2. Compiled Mechanical Properties of Bulk Fiber Layers Mimicking the Mechanical Properties of the Superficial, Middle, Deep, and Bulk Cartilage Zones

Electrospun cartilage equivalent	*Fiber size (μm)*	*Fiber orientation*	*Tensile modulus (MPa)*	*Tensile stress (MPa)*
Superficial	1	Aligned	35 ± 2	20 ± 4
Middle	1	Random	12.4 ± 4.4	7.4 ± 0.7
Deep	5	Random	7 ± 3.9	5.7 ± 0.4
Trilaminar Composite	1–5	Multi	25 ± 3	8.4 ± 1

Tensile properties decreased within each zone with respect from superficial to deep based on the orientation and size of the fiber. Tensile testing of the trilaminar composite indicated mechanical properties between those of the individual layers.

However, chondrocytes did not exhibit this alignment on either the randomly oriented fiber scaffolds or the randomly oriented zone of trilaminar scaffolds and instead exhibited spread morphologies (Fig. 2J, L).

To quantify the number of chondrocytes on fibrous scaffolds, DNA content was measured postseeding and after 1, 3, and 5 weeks in culture (Fig. 3A). Chondrocyte adhesion was not significantly different among any of the scaffold groups immediately after seeding, and in all groups, the chondrocyte number increased significantly after 1 and 3 weeks in culture. By week 5, all scaffolds demonstrated decreases in chondrocyte DNA content compared to after 1 week in culture. However, the DNA content on all scaffolds was still greater after 5 weeks than that measured immediately postseeding. Total GAG content increased between postseeding and week 1 for all groups, yet was not significantly different from one another (Fig. 3B). At weeks 3 and 5, total GAG content was significantly higher comparative to postseeding levels and 1 week of culture for all groups. GAG content normalized to DNA content significantly increased with time, but did not indicate any significant differences in GAG production per cell at any time point between the scaffold groups investigated (Fig. 3C).

Histological examination of fibrous scaffolds revealed collagen and GAGs throughout homogenous scaffolds (both aligned and randomly oriented; Fig. 4A, B, D, E), but variations in both collagen and GAG distribution in the trilaminar composite scaffolds (Fig. 4C, F) with preferential deposition in the superficial (aligned 1 μm) and deep zones (random 5 μm) were evident. Production and secretion of type II collagen were present on all scaffold types as revealed by immunohistochemical staining (Fig. 5A–D) with minimal staining for type I collagen (Fig. 5E–H).

mRNA levels of *ACAN* and *COL2A1* were also significantly increased from week 1 and up to week 5. Expression of *COL1A1* decreased after week 1 and continued to decrease

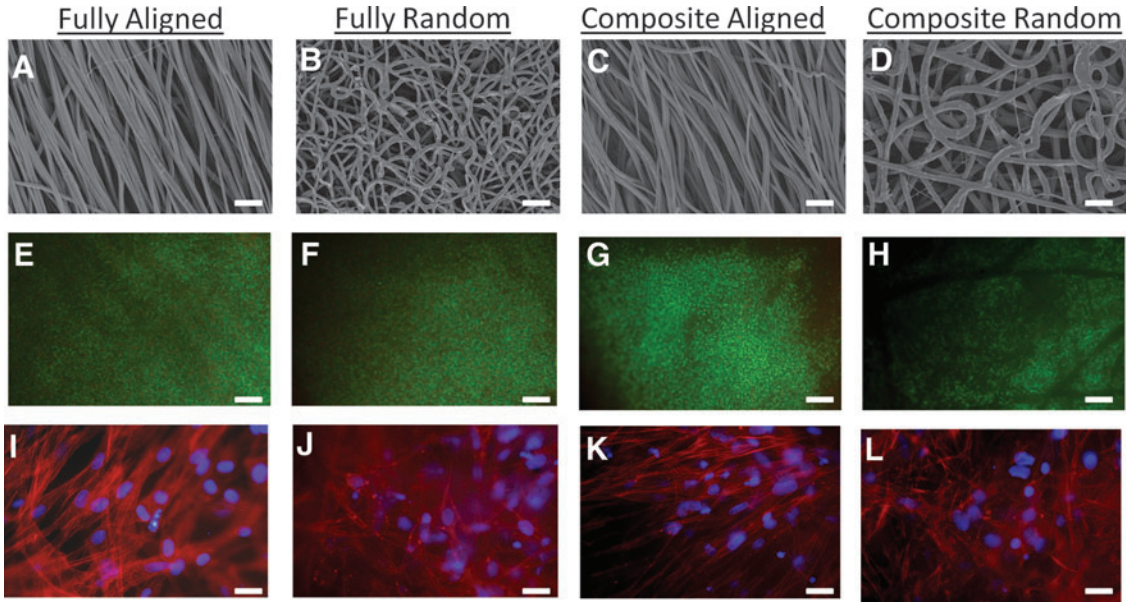

FIG. 2. Electron microscopy images of homogeneous fibrous scaffolds of either aligned **(A)** or randomly oriented fibers **(B)** and trilaminar scaffolds **(C, D)** (superficial zone = **C** and deep cartilage zone = **D**). Chondrocyte viability on homogenous fibrous scaffolds of either aligned **(E)** or randomly oriented **(F)** fiber scaffolds and on trilaminar with either aligned **(G)** or randomly oriented **(H)** fiber organizations after five weeks in culture, where live cells fluoresce green and dead cells fluoresce red. Chondrocyte morphology on homogeneous fully fibrous scaffolds of either aligned **(I)** or randomly oriented **(J)** fiber scaffolds. Chondrocytes on aligned fibers exhibited spindle-like morphologies orienting along the direction of fibers **(I)**, whereas chondrocytes on randomly oriented scaffolds displayed spread morphologies **(J)**. Chondrocytes on trilaminar scaffolds displayed different morphologies that were dependent on zone-specific fiber orientation and either aligned with fibers **(K)** or were spread **(L)**. Scale bar = 10 μm for **(A–D)** and **(I–L)**; scale bar = 100 μm for **(E–H).**

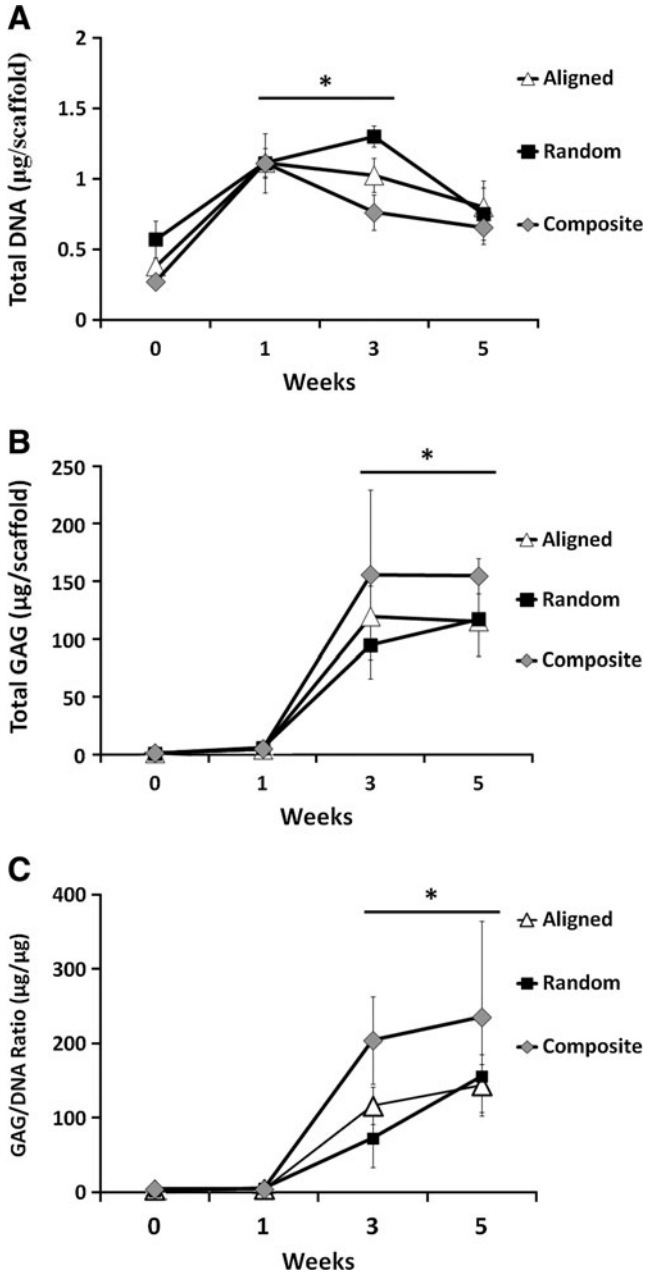

FIG. 3. DNA and glycosaminoglycan (GAG) content in chondrocyte-seeded scaffolds during the 5-week culture period. DNA content increased significantly after 1 and 3 weeks in culture, but no further increases were noted at week 5 **(A)**. GAG content significantly increased on week 3 and 5 **(B)**. Normalized GAG content displayed significant enhancements at week 3 and 5 comparative to week 1 **(C)**, indicating significant chondrocyte differentiation. *Significant difference ($p < 0.05$).

up to week 5. Furthermore, expression of *COL2A1* increased up to week 3. As a result, the ratio of expression *COL2A1/COL1A1* increased significantly during the experiment time course. Although, no significant differences were observed between the scaffold types, all scaffolds sustained chondrogenic gene expression, an indicator of maintenance of the chondrocyte phenotype (Fig. 6).

Mechanical assessment of chondrocyte-seeded scaffolds

To assess mechanical properties of scaffolds cultured with bovine chondrocytes, we performed tensile and unconfined compression analyses immediately postseeding (week 0) and after 5 weeks in culture. Tensile tests revealed maintenance of tensile properties with no significant variations after 5 weeks of culture compared to week-0 controls (Table 3). However, compressive tests did reveal significantly a different behavior after 5 weeks in culture (Table 3). The application of a 0.07N preload to scaffolds resulted in different viscoelastic behavior depending on time in culture. Week-5 scaffolds underwent stress relaxation, achieving an equilibrium force of <0.04N for all groups, whereas week-0 controls all maintained significantly higher equilibrium forces (Fig. 7). Homogenous, randomly oriented scaffolds exhibited significantly higher compressive moduli (weeks 0 and 5) compared to both homogenous aligned and trilaminar composite scaffolds with values of 511.9 ± 69 and 520.9 ± 144 kPa, respectively (Table 3). Compressive properties of homogenous aligned and trilaminar composite scaffolds were not significantly different at week 0 (136.3 ± 16.6 and 152.5 ± 42.2 kPa, respectively), and both displayed significant decreases in compressive moduli after 5 weeks in culture (52.5 ± 10.6 and 65.7 ± 27.5 kPa, respectively) compared to week-0 controls (Table 3). Compressive testing of scaffolds cultured for 5 weeks up to 30% strain yielded significant increases in compressive moduli for all fibrous scaffolds (Fig. 8). Additionally, at 10%–20% and 20%–30% strain, we noted a significant increase in the compressive properties of trilaminar composite scaffolds compared to those in the homogenous aligned group.

Discussion

Articular cartilage exhibits depth-dependent mechanical properties based on the arrangement of its extracellular matrix components, and more specifically, the varying alignment and tensile properties of its collagen fiber microstructure. Cartilage's collagen fiber arrangement supports tissue function by resisting complete compression and acting to maintain tissue integrity under dynamic compression. To recreate this structurally challenging tissue, we fabricated trilaminar composite scaffolds using the method of sequential electrospinning and created scaffolds comprised of fibers with zone-specific sizes and orientations to mimic the microstructural organization and mechanical properties of articular cartilage.

Zonal tissue engineering of articular cartilage continues to undergo significant progress, as researchers have sought to recreate the anisotropic biochemical and biomechanical properties of this tissue.[2,21,22] In particular, researchers have focused on the utilization of chondrocyte subpopulations,[23] effective changes in scaffold pore sizes, and varying scaffold matrix composition and mechanics.[24,25] In this work, we have extended this area of research by creating graded fibrous scaffolds with variations in fiber alignment and fiber size to afford a material with zonal tensile properties as well as stratified compressive mechanical properties.

As demonstrated in this work and by others, two defining features of electrospun fibrous scaffolds are fiber size and orientation, as these variables dictate bulk physical and

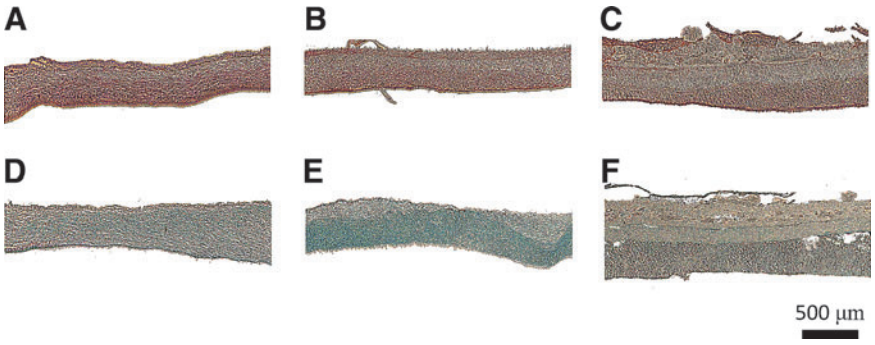

FIG. 4. Histological staining of extracellular matrix deposition in fibrous scaffold of aligned **(A, B)**, randomly oriented **(C, D)**, and trilaminar composite scaffolds **(E, F)** after 5 weeks in culture. Fibrous scaffolds were stained with Picrosirius Red for collagen content **(A, C, E)** or Alcian Blue for GAG content **(B, D, F)**. Aligned and randomly oriented fibrous scaffolds exhibited homogenous extracellular matrix deposition, whereas in trilaminar composites, matrix deposition was zone specific. Scale bar = 500 μm.

mechanical properties, as well as cellular response in terms of alignment, proliferation, and differentiation.[11,26] Here, we varied polymer concentration and collector speed to generate continuous trilaminar scaffolds that contained fibers aligned parallel to the surface, then randomly, and finally randomly, but with larger diameters, which crudely mimicked the collagen fibril arrangement and zonal tensile properties in native cartilage. Scaffolds with randomly oriented larger fibers also had larger pore sizes than those made from smaller fibers. Larger pore sizes may aid in cell infiltration and nutrient transport, as dense fiber networks created from submicron-size electrospun fibers have been shown to limit cell infiltration.[27] Such larger fiber scaffolds, however, had lower tensile properties than those created from smaller diameter fibers, which was likely due to the increased solution viscosity resulting from the higher polymer concentration. This likely impeded fiber stretching and polymer chain orientation along the length of individual fibers, reducing their tensile moduli and strengths.[11] Conversely, scaffolds created from aligned fibers had significantly higher tensile properties than those with random orientations, which likely resulted from simultaneous recruitment of highly aligned fibers during tensile loading. Trilaminar composite scaffolds yielded a significantly higher tensile modulus than randomly oriented small (1 μm) or large (5 μm) fiber diameter homogenous scaffolds, which suggests that the addition of the aligned superficial region significantly contributed to the tensile properties of the bulk scaffold. Tensile testing of cell-seeded scaffolds revealed that tensile properties were maintained throughout the culture period. We attribute the maintenance of tensile properties to 1) the brevity of the culture period (5 weeks) and 2) the slow degradation rate of PCL. Indeed, Baker and Mauck have demonstrated that time-dependent changes in the mechanical properties of fiber scaffolds made from PCL are quite limited, and are mainly acquired after extensive deposition of the extracellular matrix requiring long-term culture (10 weeks).[8]

We also examined the ability of homogenous and trilaminar fibrous scaffolds to support the formation of cartilage-like tissue *in vitro*. All scaffolds supported chondrocyte attachment and viability after up to 5 weeks in culture, demonstrating that the material system and fabricated scaffolds were biocompatible, as has been previously reported by Baker *et al*.[8] Nevertheless, the cell morphology varied depending on the fiber organization, with trilaminar scaffolds fostering aligned cell morphologies in the superficial zone and spread in the randomly oriented deep zone of the scaffold. While chondrocytes in native cartilage tend to have rounded morphologies, the addition of adsorbed proteins to scaffolds to promote cell attachment in the present study likely promoted the more spread morphologies observed here.[28] The use of fibrous scaffolds combined with hydrogels,

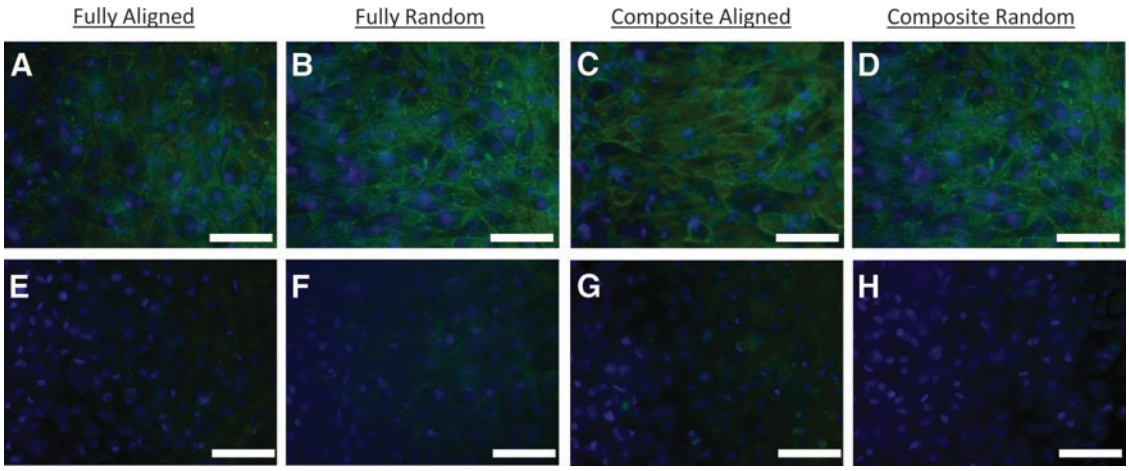

FIG. 5. Immunohistochemistry staining for type II collagen **(A–D)** and type I collagen **(E–H)** deposition in fibrous scaffold of aligned **(A, E)**, randomly oriented **(B, F)**, and trilaminar composite scaffolds **(D, F)** after 5 weeks in culture. Blue: nuclei; green: collagen type II **(A–D)** or collagen type I **(E–H)**; scale bar = 50 μm.

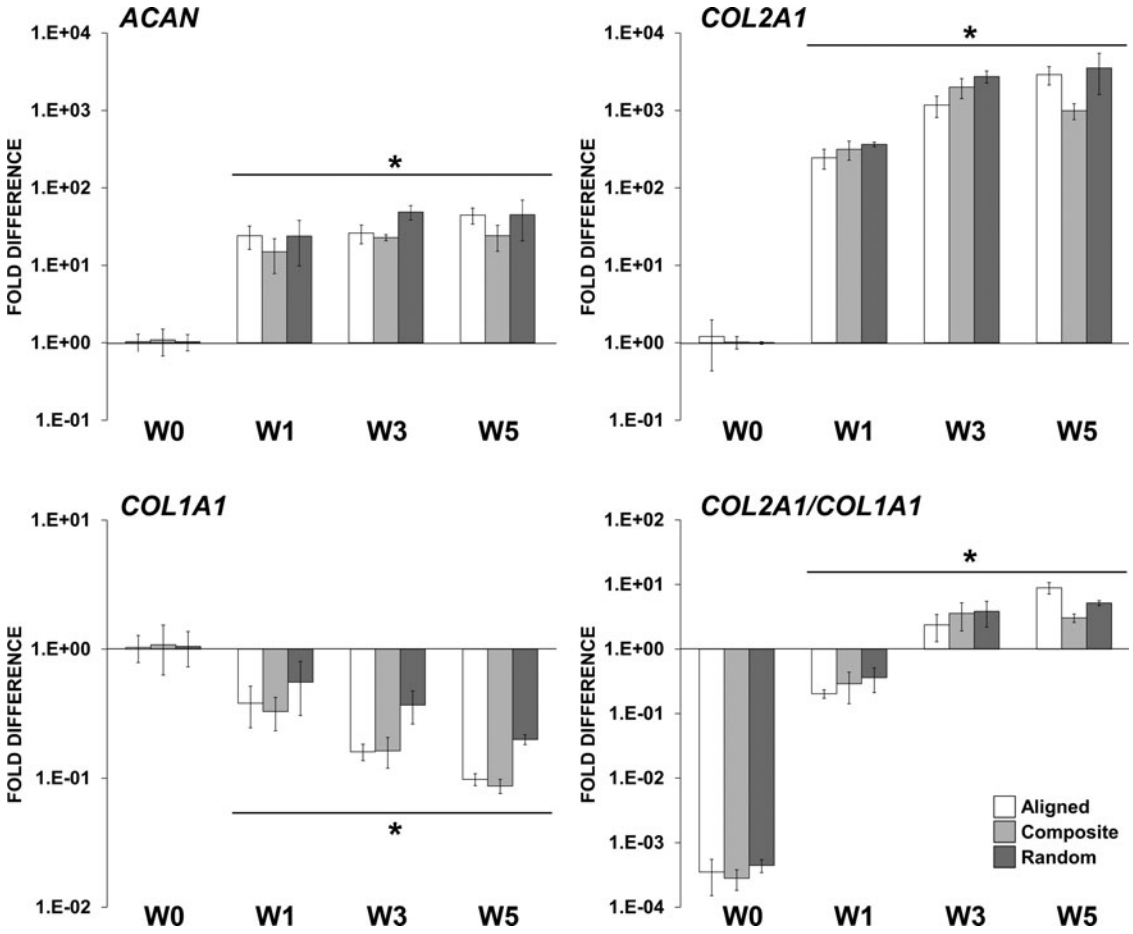

FIG. 6. Gene expression profile of bovine chondrocytes cultured on the fibrous scaffolds in a chondrogenic medium. mRNA levels of *ACAN*, *COL2A1*, and *COL1A1* are represented as fold difference relative to week-0 controls (1 day postseeding) after normalization with the housekeeping *GAPDH* gene. *Significant difference ($p < 0.05$).

as has been previously reported,[29] may preclude the need for protein adsorption on scaffolds and may be a more effective means to maintain cells with native tissue-like morphologies within fibrous scaffolds. Nevertheless, our morphological observations demonstrate that zonal variations within trilaminar scaffolds affect the cell morphology and likely function. Although not probed in this study, the scaffold morphology is known to control gene expression and therefore could enhance the expression of zonal markers, such as lubricin in the superficial zone or aggrecan within the deep zone.[3]

In addition to promoting cell attachment and viability, all scaffolds examined also supported chondrocyte proliferation and GAG production. This has been previously shown in fibrous scaffolds created for intervertebral disc repair and cartilage regeneration,[7,30] where collagen and GAG-rich extracellular matrices are deposited and maintained on fibrous PCL scaffolds *in vitro*. Production and secretion of type II collagen were present on all scaffolds with minimal staining for type I collagen. These results, associated with the highly increasing *COL2A1/COL1A1* expression level ratio over time, indicated maintenance of the chondrocyte phenotype on the fibrous scaffolds. Trilaminar scaffolds supported chondrocyte proliferation, and the production of a GAG-rich extracellular matrix that upon quantification was not significantly different from that produced in homogenous scaffolds. This demonstrates that variations in fiber orientation and size in a continuous scaffold do not impede cell attachment and proliferation or GAG production, while still providing the mechanical and morphological cues of a more native tissue-like organization. Histological analyses similarly demonstrated collagen and GAG in all scaffolds. However, while in standard aligned and randomly oriented scaffolds, collagen and GAG were homogenously distributed, in trilaminar scaffolds, more intense collagen and GAG staining were noted in the superficial and deep zones. Increased extracellular matrix production in the deep zone of trilaminar scaffolds may be attributable, at least in part, to the larger fiber diameters in this zone and resultantly larger pore sizes, which may promote increased cellularity and nutrient transport. As previously determined, varying the fiber size can influence the *in vitro* formation of cartilage by primary chondrocytes and bone marrow-derived mesenchymal stem cells.[31–33] Shamugasundaram *et al.* determined that the gene expression of aggrecan, chondroadherin, Sox 9, and collagen II were upregulated in cells on scaffolds comprised of either 5- or 9-μm-diameter fibers, an effect they attributed to the larger pores that afforded space for cellular aggregation.[31] In contrast, Wise *et al.* and Li *et al.* have similarly noted differences in chondrogenesis, where both report

Table 3. Compiled Tensile and Compressive Mechanical Properties of the Cell-Seeded Scaffolds at Week 0 and 5

	Week 0		*Week 5*	
Electrospun cartilage equivalent	*Tensile modulus (MPa)*	*Tensile stress (MPa)*	*Tensile modulus (MPa)*	*Tensile stress (MPa)*
Aligned	35 ± 2	20 ± 4	43 ± 5	23 ± 3
Random	12.4 ± 4.4	7.4 ± 0.7	15 ± 2.7	5 ± 3.7
Trilaminar composite	25 ± 3	8.4 ± 1	22 ± 6.1	7 ± 0.4
	Week 0		*Week 5*	
Electrospun cartilage equivalent	*Compressive modulus (kPa)*	*Compressive stress (kPa)*	*Compressive modulus (kPa)*	*Compressive stress (kPa)*
Aligned	136.3 ± 16.6	22.5 ± 2.5	52.5 ± 10.6	8.1 ± 2
Random	511.9 ± 69	61.9 ± 7	520.9 ± 144	58 ± 16.1
Trilaminar composite	152.5 ± 42.2	23.1 ± 4.5	65.7 ± 27.5	9.7 ± 4.4
	Excised tissue			
	Compressive modulus (kPa)		*Compressive stress (kPa)*	
Native cartilage	89.5 ± 48.6		14.5 ± 5.3	

A 5-week growth period did not significantly affect the tensile properties, yet the compressive properties of the aligned and the trilaminar composite scaffold were significantly different with average stiffness reductions of 84 and 87 kPa, respectively. The random scaffold displayed no significant difference in stiffness. The stiffness values found for the native cartilage compare favorably with the 5-week growth period for the aligned and composite scaffolds.

that smaller fiber diameters supported more normal chondrocyte morphology and matrix production.[32,33] Thus, the role of fiber size seems to be dependent on the cell type, culture condition, and scaffold chemistry.

Additionally, the ability of cells to fully colonize multilayered electrospun scaffolds comprised of varying fiber orientation is an area that has not been fully addressed,[30] as variations in fiber orientation from aligned to random networks may also prove to be limiting in terms of cell migration and subsequent colonization. In addition to gradations in fiber orientation, cellular colonization has been shown to be improved with longer culture times and dynamic culture conditions.[20] Inclusion of porogenic materials, specifically dissolvable polymer fibers, may be required to increase the resultant pore size and cellular colonization within the fibrous scaffold.[27] Taken together, these data suggest that depth-dependent variation in fiber size and orientation influence extracellular matrix deposition and organization, producing engineered scaffolds with more similarities to native cartilage than that observed in homogenous scaffolds.

Chondrocyte culture within an appropriate three-dimensional microenvironment that provides appropriate biochemical cues for differentiation (such as TGF-β1/3) has been shown to promote the production of a cartilage-like extracellular matrix,[34] which includes an abundance of hydrophilic sulfated GAG. Here, we report that the application of a preload to scaffolds cultured for 5 weeks resulted in significant relaxation of the scaffolds. Native cartilage is

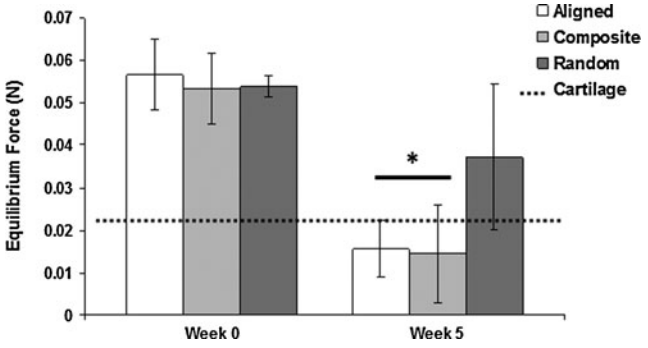

FIG. 7. Equilibrium load attained after a 5-min preload of 0.07N. After five weeks in culture, aligned and trilaminar scaffold groups showed significant decreases in the equilibrium force compared to week-0 controls and were more similar to equilibrium forces measured in native cartilage. *Significant difference ($p < 0.05$).

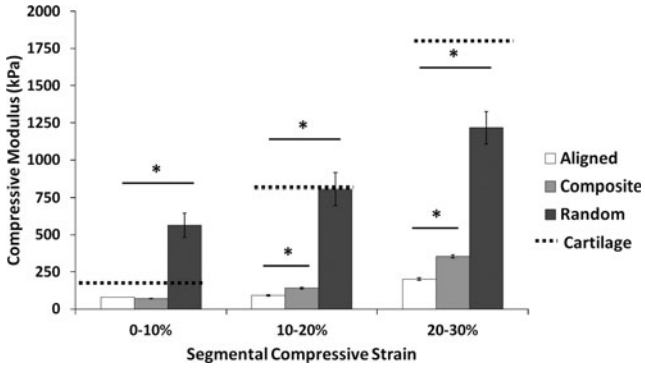

FIG. 8. Segmental compressive moduli of fibrous scaffolds after 5 weeks in culture. At higher strain rates, significant differences were noted for all scaffold types, and at the higher strain rates, trilaminar composite scaffold exhibited significant increases in compressive moduli compared to aligned fibrous scaffolds. *Significant difference ($p < 0.05$).

known to undergo stress relaxation in unconfined compression, as fluid associated with GAG is squeezed out of the tissue.[35] Similar viscoelastic behavior in the scaffolds examined here suggests that the production of GAG by constituent cells promotes more native tissue-like time-dependent behavior compared to cell-free scaffolds.

While 5 weeks in culture promoted more cartilage-like viscoelastic behavior, surprisingly, the compressive moduli and peak stress of cultured scaffolds were significantly lower than those of week-0 controls. As histological staining and biochemical assays demonstrated increased extracellular matrix production in cultured scaffolds, which should only have increased the mechanical properties of cultured scaffolds, it is possible that the lower mechanical properties may have resulted, because the fibrous scaffold itself underwent some degree of degradation. Although PCL does not undergo significant enzymatic degradation *in vitro*,[36] acidic byproducts of cellular metabolism in the static culture system employed here may have contributed to a small degree of degradation in the randomly oriented portions of the polymer scaffold, perhaps specifically targeting fiber interstices. Conversely, the addition of GAG to the surface of fibrous scaffolds could have mediated this change in a mechanical behavior. Moutos and Guilak noted that the compressive mechanical properties of cell-seeded fiber-reinforced scaffolds were reduced compared to acellular controls.[37] They hypothesized that the lower mechanical properties may have stemmed from increased accumulation of neotissue along the outer surfaces of the scaffold, which acted as a deformable layer that effectively reduced the apparent stiffness of the entire structure.[37] Here, extracellular matrix accumulation on the surface of the cell-seeded scaffolds may have similarly caused an effective reduction in scaffold stiffness.

Despite the significant decreases in compressive properties noted here in both homogenous and trilaminar scaffolds after long-term culture, the mechanical properties of trilaminar scaffolds were not significantly different from those observed in native cartilage up to 10% strain. While our results demonstrate that homogenous, aligned fibrous scaffolds were relatively weaker than randomly oriented scaffolds, the compressive properties of the trilaminar composites, which were intermediate of the two, closely approximated those of the native tissue. These differences can be explained by the fiber structure, with aligned scaffolds possessing slip planes between each fiber, while the randomly oriented scaffolds have fiber crossovers, which resist compression by reinforcing the bulk scaffold. Poor solvent evaporation or solvent retention within the randomly oriented scaffolds (some welded fibers were observed under SEM) most likely further contributed to this phenomenon, as the relatively low linear velocity (0–1 m/s) of the collector made less of a contribution to fiber drying and solvent evaporation compared to the aligned fiber scaffolds.

When testing under physiological strains up to 10%, we noted no differences in the compressive properties of trilaminar composite and aligned fiber scaffolds. As the trilaminar composite scaffolds were comprised of approximately one-third aligned fibers, however, we hypothesize that we were preferentially testing the aligned portion of the scaffolds. When we tested scaffolds at up to 30% strain and determined the segmental modulus, we found significant increases in trilaminar composite scaffolds at 20% and 30% strains. These results further demonstrate that the trilaminar composite design offers distinct advantages over homogenous designs in terms of mechanical properties and cellular behavior in terms of morphological organization, while not adversely affecting extracellular matrix production.

Conclusions

To our knowledge, this is the first work that has created trilaminar fibrous scaffolds to mimic the organization and zonal tensile properties of articular cartilage. Such scaffolds supported the production of cartilage-like extracellular matrix as has been previously reported in homogenous electrospun scaffolds, but with a depth-dependent organization. Taken together, our results suggest that fibrous scaffolds inspired by the structural organization of the native tissue may find use in developing regenerative medicine strategies to treat articular cartilage lesions.

Acknowledgments

The authors would like to thank Ms. Sabrina Skeete for laboratory assistance, Dr. Sandra Shelfelbine for the use of the Instron mechanical tester, and Prof. Charles Archer and Dr. Ilyas Khan for their advice with regard to the chondrocyte isolation. M.M.S acknowledges the Medical Engineering Solutions in Osteoarthritis Centre of Excellence funded by the Wellcome Trust and the EPSRC for the funding of SDMcC and HA. A.C. thanks the Irish Research Council for Science, Engineering and Technology (IRCSET)–Marie Curie International Mobility Fellowship co-funded grant PD/2010/INSP/1948 for funding.

Disclosure Statement

No competing financial interests exist.

References

1. Daher, R.J., Chahine, N.O., Greenburg, A.S., Sgagilone, N.A., and Grande, D.A. New methods to diagnose and treat cartilage degeneration. Nat Rev Rheumatology **5,** 599, 2009.
2. Klein, T.J., Malda, J., Sah, R.L., and Hutmacher, D.W. Tissue engineering of articular cartilage with biomimetic zones. Tissue Eng **15,** 143, 2009.
3. Becerra, J., Andrades, J.A., Guerado, E., Zamora-Navas, P., Lopez-Puertas, J.M., and Reddi, H. Articular cartilage: structure and regeneration. Tissue Eng Part B **16,** 617, 2010.
4. Erggelet, C., Kreuz, P.C., Mrosek, E.H., Schagemann, J.C., Lahm, A., Ducommun, P.P., *et al.* Autologous chondrocyte implantation versus ACI using 3D-bioresorbably graft for the treatment of large full-thickness cartilage lesions of the knee. Arch Orthop Trauma Surg **130,** 957, 2010.
5. Nuernberger, S., Cyran, N., Albrecht, C., Redl, H., Vecsei, V., and Marlovits, S. The influence of scaffold architecture on chondrocyte distribution and behavior in matrix-associated chondrocyte transplantation grafts. Biomaterials **32,** 1032, 2011.
6. da Silva, M.L.A., Martins, A., Costa-Pinto, A.R., Costa, P., Faria, S., Gomes, M., *et al.* Cartilage tissue engineering using electrospun PCL nanofiber meshes and MSCs. Biomacromolecules **11,** 3228, 2010.
7. Baker, B.M., Nathan, A.S., Gee, A.O., and Mauck, R.L. The influence of an aligned nanofibrous topography on human mesenchymal stem cell fibrochondrogenesis. Biomaterials **31,** 6190, 2010.

8. Baker, B.M., and Mauck, R.L. The efffect of nanofiber alignment on the maturation of engineered meniscus constructs. Biomaterials **28,** 1967, 2007.
9. Mauck, R.L., Baker, B.M., Nerurkar, N.L., Burdick, J.A., Li, W.J., Tuan, R.S., *et al.* Engineering on the straight and narrow: The mechanics of nanofibrous assemblies of fiber-reinforced tissue regeneration. Tissue Eng Part B Rev **15,** 171, 2009.
10. Kwon, I.K., Kidoaki, S., and Matsuda, T. Electrospun nano- to microfiber fabrics made of biodegradable copolyesters: structural characteristics, mechanical properties, and cell adhesion potential. Biomaterials **26,** 3929, 2005.
11. Ju, Y.M., Choi, J.S., Atala, A., Yoo, J.J., and Lee, S.J. Bilayered scaffold for engineering cellularized blood vessels. Biomaterials **31,** 4313, 2010.
12. Teo, W.E., and Ramakrishna, S. Electrospun nanofibers as a platform for multifunctional, hierarchically organized nanocomposite. Comp Sci Technol **69,** 1804, 2009.
13. Nerurkar, N.L., Elliot, D.M., and Mauck, R.L. Mechanics of oriented electrospun nanofibrous scaffolds for annulus fibrous tissue engineering. J Orthop Res **25,** 1018, 2007.
14. Woodfield, T.B.F., Van Blitterswijk, C.A., De Wijn, J., Sims, T.J., Hollander, A.P., and Riesle, J. Polymer scaffolds fabricated with pore-size gradients as a model for studying the zonal organization within tissue-engineered cartilage constructs. Tissue Eng **11,** 1297, 2005.
15. Moutos, F.T., Free, L.E., and Guilak, F. A biomimetic three-dimensional woven composite scaffold for functional tissue engineering of cartilage. Nat Mater **6,** 162, 2007.
16. Erisken, C., Kalyon, D.M., and Wang, H. Functionally graded electrospun polycaprolactone and beta-tricalcium phosphate nanocomposites for tissue engineering applications. Biomaterials **29,** 4065, 2008.
17. Kidoaki, S., Kwon, I.K., and Matsuda, T. Mesoscopic spatial designs of nano- and microfiber meshes for tissue-engineering matrix and scaffold based on newly devised multilayering and mixing electrospinning techniques. Biomaterials **26,** 37, 2005.
18. Lee, S.J., Liu, J., Oh, S.H., Soker, S., Atala, A., and Yoo, J.J. Development of a composite vascular scaffolding system that withstands physiological vascular conditions. Biomaterials **29,** 2891, 2008.
19. McClure, M.J., Sell, S.A., Simpson, D.G., Walpoth, B.H., and Bowlin, G.L. A three-layered elecrospun matrix to mimic native arterial architecture using polycaprolactone, elastin, and collagen: a preliminary study. Acta Biomater **6,** 2422, 2010.
20. Nerurkar, N.L., Sen, S., Baker, B.M., Elliot, D.M., and Mauck, R.L. Dynamic culture enhances stem cell infiltration and modulates extracellular matrix production on aligned electrospun nanofibrous scaffolds. Acta Biomater **7,** 485, 2011.
21. Klein, T.J., Rizzi, S.C., Reichert, J.C., Georgi, N., Malda, J., Schuurman, W., *et al.* Strategies for zonal cartilage repair using hydrogels. Macromol Biosci **9,** 1049, 2009.
22. Klein, T.J., Chaudhry, M., Bae, W.C., and Sah, R.L. Depth-dependent biomechanical and biochemical properties of fetal, newborn, and tissue-engineered articular cartilage. J Biomech **40,** 182, 2007.
23. Ng, K.W., Ateshain, G.A., and Hung, C.T. Zonal chondrocytes seeded in a layered agarose hydrogel create engineered cartilage with depth-dependent cellular and mechanical inhomogeneity. Tissue Eng Part A **15,** 2315, 2009.
24. Tang, Y., Wong, C., Wang, H., Sutti, A., Kirkland, M., Wang, X., *et al.* Three-dimensional tissue scaffolds from interbonded poly(e-caprolactone) fibrous matrices with controlled porosity. Tissue Eng Part C Methods **17,** 209, 2011.
25. Nguyen, L.H., Kudva, A.K., Saxena, N.S., and Roy, K. Engineering articular cartilage with spatially-varying matrix composition and mechanical properties from a single stem cell population using a multi-layered hydrogel. Biomaterials **32,** 6946, 2011.
26. Wong, S.C., Baji, A., and Leng, S. Effect of fiber diameter on tensile properties of electrospun poly(e-caprolactone). Polymer **49,** 4713, 2008.
27. Baker, B.M., Gee, A.O., Metter, R.B., Nathan, A.S., Marklein, R.A., Burdick, J.A., *et al.* The potential to improve cell infiltration in composite fiber-aligned electrospun scaffolds by the selective removal of sacrificial fibers. Biomaterials **29,** 2348, 2008.
28. Schagemann, J.C., Kurz, H., Casper, M.E., Stone, J.S., Dadsetan, M., Yu-Long, S., *et al.* The effect of scaffold composition on the early structural characteristics of chondrocytes and expression of adhesion molecules. Biomaterials **31,** 2798, 2010.
29. Ekaputra, A.K., Prestwich, G.D., Cool, S.M., and Hutmacher, D.W. Combining electrospun scaffolds with electrosprayed hydrogels leads to three-dimensional cellularization of hybrid constructs. Biomacromolecules **9,** 2097, 2008.
30. Pham, Q.P., Sharma, U., and Mikos, A.G. Electrospun poly(e-caprolactone) microfiber and multilayer nanofiber/microfiber scaffolds: characterization of scaffolds and measurement of cellular infiltration. Biomacromolecules **7,** 2796, 2006.
31. Shanmugasundaram, S., Chaudhry, H., and Arinzeh, T.L. Microscale versus nanoscale scaffold architecture for mesenchymal stem cell chondrogenesis. Tissue Eng Part A **17,** 831, 2011.
32. Wise, J.K., Yarin, A.L., Megaridis, C.M., and Cho, M. Chondrogenic differentiation of human mesenchymal stem cells on oriented nanofibrous scaffolds: engineering the superficial zone of articular cartilage. Tissue Eng Part A **15,** 913, 2009.
33. Li, W.J., Jiang, Y.J., and Tuan, R.S. Chondrocyte phenotype in engineered fibrous matrix is regulated by fiber size. Tissue Eng **12,** 1775, 2006.
34. Barry, F., Boynton, R.E., Liu, B.S., and Murphy, J.M. Chondrogenic differentiation of mesenchymal stem cells from bone marrow: differentiation-dependent gene expression of matrix components. Exp Cell Res **268,** 189, 2003.
35. Freeman, M.A.R., editor. Adult Articular Cartilage, 2nd ed. Kent, England: Pitman Medical, 1979.
36. Woodruff, M.A., and Hutmacher, D.W. The return of a forgotten polymer-polycaprolactone in the 21st century. Progr Polym Sci **35,** 1217, 2010.
37. Moutos, F.T., and Guilak, F. Functional properties of cell-seeded three-dimensionally woven poly(e-caprolactone) scaffolds for cartilage tissue engineering. Tissue Eng Part A **16,** 1291, 2010.

Address correspondence to:
Molly M. Stevens, Ph.D.
Departments of Materials and Bioengineering
Institute of Biomedical Engineering
Imperial College London
London SW7 2AZ
United Kingdom

E-mail: m.stevens@imperial.ac.uk

Received: October 24, 2011
Accepted: May 30, 2012
Online Publication Date: July 31, 2012